

# Dynamic Light Scattering from Dilute, Semidilute, and Concentrated Block Copolymer Solutions

C. Pan,<sup>†</sup> W. Maurer,<sup>‡</sup> Z. Liu, and T. P. Lodge\*

Department of Chemistry, University of Minnesota, Minneapolis, Minnesota 55455-0431

P. Stepanek

Institute of Macromolecular Chemistry, Czech Academy of Sciences, Prague, Czech Republic

E. D. von Meerwall

Department of Physics and Institute for Polymer Science, University of Akron, Akron, Ohio 44325

H. Watanabe<sup>§</sup>

Department of Macromolecular Science, Osaka University, Osaka, Japan

Received June 7, 1994; Revised Manuscript Received October 19, 1994\*

**ABSTRACT:** The dynamic light scattering (DLS) properties of four symmetric polystyrene–polyisoprene diblock copolymers have been examined in the neutral good solvent toluene. Concentrations ( $c$ ) ranged from the dilute, through the semidilute, and into the concentrated regimes. Pulsed-field-gradient NMR has been used to determine the translational diffusivities ( $D_s$ ) of the same copolymers, at selected concentrations. The results are in substantial agreement with models developed by Benmouna and co-workers and by Semenov. Three modes are predicted: cooperative diffusion ( $D_C$ ), corresponding to relaxation of fluctuations in polymer concentration; an internal mode ( $\Gamma_I$ ), reflecting relative motion of the two blocks within one molecule; a heterogeneity mode ( $D_H$ ), due to chain-to-chain fluctuations in composition and which relaxes by translational diffusion. In dilute solutions, a single, diffusive mode is seen and is attributed to a superposition of  $D_C$  and  $D_H$ . In semidilute and concentrated solutions,  $D_C$  and  $D_H$  are cleanly resolved.  $D_C$  shows the expected scaling with  $c$  and molecular weight ( $M$ ), i.e.,  $D_C \sim c^{0.7}M^0$ . Comparison with the NMR results confirms that the values of the diffusion coefficients  $D_H$  and  $D_s$  are very similar; this result extends the previous work of Balsara and co-workers, who first noted the appearance of a block copolymer DLS mode resembling translational diffusion. Selected measurements in two other good solvents, THF and chloroform, establish that  $D_C$  and  $D_H$  are independent of solvent refractive index ( $n_s$ ), as expected. The relative amplitudes of the cooperative and heterogeneity modes also scale with  $c$ ,  $M$ , and  $n_s$  in agreement with theory. The predicted internal mode is generally difficult to resolve but is seen for the highest molecular weight sample examined. The concentration dependences of  $D_H$  and  $D_s$  are insensitive to the order–disorder transition, in agreement with previous measurements in solutions and melts. Preliminary measurements of  $D_H$  with a novel Fourier transform heterodyne DLS apparatus were also in good agreement with the other techniques. Finally, the results are compared with previous DLS measurements of symmetric diblock copolymers in solution. It is proposed that the apparent discrepancies among the previous studies can be resolved, by appropriate assignment of the heterogeneity mode.

## Introduction

The properties of block copolymers in the vicinity of the order–disorder transition (ODT) have proven to be remarkably rich. For example, in the disordered state but near the transition, there is evidence of significant non-mean-field behavior, such as chain stretching<sup>1</sup> and large-amplitude concentration fluctuations.<sup>2,3</sup> Similarly, in the ordered state several novel morphologies have recently been uncovered,<sup>4–6</sup> to complement the well-known lamellar, cylindrical, and spherical microphases. The boundaries between these structures appear to depend sensitively on subtle effects, including chain stretching, fluctuations, and chain stiffness asymmetry. Consequently, it is of particular interest to

explore the dynamics in such systems. One promising strategy is to utilize block copolymers in a neutral (i.e., nonselective) good solvent and to vary the total polymer concentration,  $c$ . In this way, the ODT can be approached systematically, even for high molecular weight chains, and the problem of a limited accessible temperature window, often encountered in melts, can be circumvented.

Dynamic light scattering (DLS) has proven to be a powerful tool in elucidating the dynamics of polymer liquids, particularly dilute and semidilute solutions.<sup>7,8</sup> DLS is sensitive to spontaneous fluctuations in the polarizability of the medium, which, for the systems of interest, are usually dominated by fluctuations in concentration. Thus, information is gained about the dynamic structure factor,  $S(q,t)$ , with the typical time window being  $10^{-6}$ – $10^2$  s. In a homogeneous, incompressible binary fluid, there is only one composition variable, and the field autocorrelation function ( $g^{(1)}(q,t) = S(q,t)/S(q,0)$ ) is usually a single-exponential decay (or distribution of exponentials, in the case of a polydisperse sample). For multicomponent systems, such as block copolymer solutions, the complexity increases, and a

\* To whom correspondence should be addressed.

<sup>†</sup> Current address: Intel Corporation, Santa Clara, CA 95052-8126.

<sup>‡</sup> Current address: Department of Chemical Engineering & Materials Science, University of Minnesota, Minneapolis, MN 55455.

<sup>§</sup> Current address: Institute for Chemical Research, Kyoto University, Uji, Kyoto-fu 601, Japan.

\* Abstract published in *Advance ACS Abstracts*, February 1, 1995.

variety of decay modes are possible.

In this paper we report measurements of the DLS from solutions containing nearly-symmetric (*i.e.*,  $f \approx 0.5$ , where  $f$  is the weight fraction of the first block in the copolymer) diblock copolymers in a neutral solvent, as a function of molecular weight and  $c$ . The specific system is polystyrene-polyisoprene in toluene; four samples, with total molecular weights ranging from  $3.5 \times 10^4$  to  $3.4 \times 10^5$ , were examined. The concentrations range from the dilute ( $c < c^*$ ), through the semidilute ( $c^* < c < 0.1$  g/mL), and into the concentrated regime ( $c > 0.1$  g/mL), and for all samples the ODT was attained. In addition to DLS, pulsed-field-gradient NMR was employed to determine the translational diffusivities of the chains. The results are compared with two complementary theoretical approaches. The first, due to Benmouna *et al.*,<sup>9,10</sup> builds on the linear response formalism for multicomponent systems of Akcasu *et al.*<sup>11,12</sup> and utilizes a dynamical mean-field (random-phase approximation) assumption. Two dynamic modes are predicted: a cooperative diffusion mode, reflecting relaxation of fluctuations in  $c$ , and an internal chain mode, arising from relative motions of the two blocks. The second theory, due to Semenov,<sup>13</sup> introduces a third mode, which is governed by the translational diffusion of the chains. This mode arises from compositional heterogeneity, *i.e.*, fluctuations in  $f$  from chain to chain, which permits fluctuations in the relative block concentration of arbitrarily long wavelength (*i.e.*,  $q \rightarrow 0$ ). This mode also could be anticipated on the basis of the previous work<sup>9-12</sup> and is analogous to the polydispersity mode described by Pusey *et al.*<sup>14</sup> for hard spheres.

The DLS from solutions of symmetric diblocks in a neutral solvent has been reported by several other workers.<sup>15-22</sup> The number of modes observed, and their identification, differed significantly. A primary reason for this complexity was that only the cooperative and internal modes were anticipated, whereas the data were not consistent with this picture. The work by Balsara *et al.*<sup>16</sup> was unique among these studies in that one of the modes was identified as translational diffusion. The subsequent explanation of this observation by Semenov *et al.*<sup>13</sup> represents a significant advance, as we feel it is now possible to reconcile almost all of these earlier, apparently disparate observations. In addition, a similar mode in copolymer melts, previously identified as "pattern relaxation",<sup>23-25</sup> has now been assigned to the heterogeneity mode.<sup>26,27</sup> In many cases, both solutions and melts, a fourth mode, slower than all of the three predicted modes, has been detected;<sup>16-21,23-27</sup> this mode has been variously ascribed to internal motions of large lamellar grains, diffusion of clusters or aggregates of chains, or long-ranged density fluctuations.

The remainder of this paper is organized as follows. In the next section, the theoretical predictions are briefly reviewed. Then, our experimental procedures and results are presented, followed by a comparison with the theories. Finally, we compare our results with those of the previous studies and offer a reinterpretation of some of the earlier data.

## Background

The predictions for the amplitudes ( $A$ ) and decay rates ( $\Gamma$ ) of the three modes identified in the Introduction are recalled here. For simplicity, a variety of assumptions are made. These include the following:

(i) The copolymers are sufficiently small that  $qR_g \ll 1$ .

(ii) The copolymers are exactly symmetric ( $f = 0.50$ ), with equal segment volumes, persistence lengths, and friction factors.

(iii) The solvent is neutral and good for both blocks, with the Flory exponent  $\nu = 0.6$ . The resulting expression for the dynamic structure factor is taken to be:

$$\frac{S(q,t)}{S(q,0)} = A_I \exp(-\Gamma_I t) + A_C \exp(-\Gamma_C t) + A_H \exp(-\Gamma_H t) \quad (1)$$

where the subscripts I, C, and H denote the internal, cooperative, and heterogeneity modes, respectively.

**Internal Mode.** This mode reflects the relative motion of the centers of mass of the two blocks on a single chain.<sup>9,10,13</sup> To within a constant of order unity,

$$\Gamma_I \approx \tau_1^{-1} \quad (2)$$

where  $\tau_1$  is the longest viscoelastic relaxation time of the chain. In particular,  $\Gamma_I$  is independent of  $q$  (for  $qR_g \ll 1$ ), as it involves motions that are independent of the observation length scale. Semenov<sup>13</sup> derived a concentration dependence for  $\Gamma_I$  in the semidilute regime, based on the blob model combined with either Rouse or reptation dynamics, but in general one does not observe either a clear Rouse-like or reptation-like regime in semidilute solutions, particularly for moderate molecular weight polymers. Thus, it is probably more appropriate to determine  $\tau_1(c)$  directly via viscoelastic or flow birefringence measurements or to estimate its concentration dependence on the basis of established empirical relations such as<sup>28,29</sup>

$$\tau_1 \approx \tau_1(c=0) \exp(\alpha c[\eta]) \quad (3)$$

where  $[\eta]$  is the intrinsic viscosity and  $\alpha$  is a parameter of order 0.4. Alternatively, one may estimate  $\Gamma_I$  relative to  $\Gamma_H$ , by an approach to be described subsequently. The amplitude of the internal mode scales as

$$A_I \propto (n_A^2 - n_B^2)^2 c^x N (qR_g)^2 \quad (4)$$

where  $n_A$  and  $n_B$  are the refractive indices of the A and B blocks,  $N$  is the total degree of polymerization, and  $x = 1$  (dilute solutions) or 0.75 (semidilute solutions). Note that  $A_I$  is proportional to  $(qR_g)^2$  and thus is expected to be small for the block copolymers examined here.

**Cooperative Mode.** This mode is essentially identical to that observed in homopolymer solutions and is thus, at least to a first approximation, independent of the copolymer nature of the chain.<sup>9,10,13</sup> In dilute solution,

$$\Gamma_C = q^2 D_C = q^2 D_0 (1 + k_d c + \dots) \quad (5)$$

whereas in the semidilute regime

$$\Gamma_C = q^2 \frac{kT}{6\pi\eta_s \xi} \propto c^{0.75} \quad (6)$$

where  $\xi$  is the correlation length and  $\eta_s$  is the solvent viscosity. The amplitude scales as

$$A_C \propto (\langle n \rangle^2 - n_s^2) c N \quad (7)$$

in dilute solution, and

$$A_C \propto (\langle n \rangle^2 - n_s^2)cg \propto (\langle n \rangle^2 - n_s^2)c^{-0.25} \quad (8)$$

in semidilute solutions, where  $\langle n \rangle$  is the average refractive index of the copolymer,  $n_s$  is the solvent refractive index, and  $g$  is the number of monomers per blob. This mode reflects mutual diffusion of the polymer and solvent, with the amplitude and rate increasing with  $c$  in the dilute regime but the amplitude decreasing with  $c$  in the semidilute regime. Note that the amplitude of this mode can be modulated by varying  $n_s$  for a given copolymer and that, for the particular choice  $\langle n \rangle = n_s$ , the "zero-average-contrast" condition,  $A_C$  should vanish.

**Heterogeneity Mode.** For perfectly monodisperse block copolymers of constant composition,  $S(q=0) = 0$ , due to the connectivity of the two blocks. However, for a finite degree of compositional heterogeneity among the chains, fluctuations in the relative concentration of A and B segments can exist at all wavelengths, even if there was no polydispersity in the total molecular weight. For  $qR_g < 1$  such fluctuations will relax by exchange of the A-rich and B-rich chains, *i.e.*, by translational diffusion. Hence, we term this the "heterogeneity mode", whereas Semenov<sup>13</sup> and Jian *et al.*,<sup>19</sup> termed it the "polydispersity mode". It is not trivial to measure the compositional heterogeneity in a block copolymer directly, but for anionically-synthesized, narrow molecular weight distribution samples, Semenov<sup>13</sup> made the reasonable assumption that the polydispersities of the two blocks were statistically independent, leading to a polydispersity factor,  $\kappa$ , given by

$$\kappa \equiv 2\delta \frac{f^2(1-f)^2}{f^2 + (1-f)^2} \quad (9)$$

where  $\delta + 1 = (M_w/M_n)$ . The resulting predictions for  $\Gamma_H$  and  $A_H$  are (with  $\nu = 0.6$ )

$$\Gamma_H = q^2 D(c, N) (1 - 2\kappa\chi N\phi^{1.53}) \quad (10)$$

and

$$A_H \propto (n_A^2 - n_B^2)^2 \frac{\kappa Nc}{1 - 2\kappa\chi N\phi^{1.53}} \quad (11)$$

in the semidilute regime; in the dilute regime, this mode should merge with the cooperative mode and become unresolvable. In eqs 10 and 11,  $\chi$  is the Flory-Huggins parameter between the A and B segments,  $D(c, N)$  is the translational diffusion coefficient of the chains, and  $\phi$  is the polymer volume fraction. It is acceptable for narrow distribution samples to assume that  $D$  is independent of fluctuations in  $f$ . Semenov<sup>13</sup> inserted the Rouse and reptation limiting expressions for  $D$  into eq 10, but, as with the longest relaxation time, it is not generally the case that the experimentally-observed dynamics follow either of these mechanisms in the semidilute regime. In particular, it has been well-documented that the molecular weight exponent for  $D$  decreases smoothly from *ca.*  $-\nu$  in dilute solutions, through the Rouse-like  $-1$  and the reptation-like  $-2$ , to values in the range  $-2.3$  to  $-2.8$ , as  $c$  is increased into the well-entangled regime.<sup>30-32</sup> Consequently, it is more appropriate to determine  $D$  directly by some other technique, such as pulsed-field-gradient NMR, in order to compare eq 10 with the DLS results.

The above analysis in general, and eq 1 in particular, amounts to identifying  $\Gamma_L$ ,  $\Gamma_C$ , and  $\Gamma_H$  as eigenvalues of a  $3 \times 3$  relaxation matrix and the corresponding

Table 1. Sample Characteristics

sample	$M_w(\text{PS})$	$M_w(\text{PI})$	$M_w/M_n$	$f_{\text{PS}}$	$R_h$ , nm
SI(16-19)	$1.6 \times 10^4$	$1.9 \times 10^4$	1.06	0.46	4.6
SI(41-45)	$4.1 \times 10^4$	$4.5 \times 10^4$	1.06	0.48	8.5
SI(73-73)	$7.3 \times 10^4$	$7.3 \times 10^4$	1.05	0.50	10
SI(170-170)	$1.7 \times 10^5$	$1.7 \times 10^5$	1.08	0.50	16

dynamic processes as the eigenvectors. However, as pointed out particularly by Akcasu *et al.*,<sup>33,34</sup> these modes need not, in general, be the eigenmodes, as some coupling can be expected. Furthermore, the simplifying assumptions listed before eq 1 are unlikely to be satisfied exactly (particularly (ii) for PS-PI). Then, even for the highest quality data, Laplace inversion of experimental correlation functions is a delicate process, and precise values of  $A$  and  $\Gamma$  cannot be expected when two or more modes are present. Thus, on both theoretical and experimental grounds, one should not necessarily anticipate quantitative agreement between the data and the above predictions.

## Experimental Section

**Samples.** Three polystyrene (PS)-polyisoprene (PI) diblock copolymers were synthesized by anionic polymerization, using *s*-butyllithium as the initiator and benzene as the solvent. The resulting values of  $M_w$  were  $3.5 \times 10^4$ ,  $8.6 \times 10^4$ , and  $3.4 \times 10^5$ , and the corresponding values of  $f$  (weight fraction PS) were 0.46, 0.48, and 0.50. These samples were designated SI(16-19), SI(41-45), and SI(170-170). A fourth sample was provided by Dr. L. J. Fetters, with  $M_w = 1.5 \times 10^5$  and  $f = 0.50$ ; it was designated SI(73-73). The sample characteristics are summarized in Table 1. Spectrograde toluene was obtained from Fisher and used as received. Some measurements were also made in HPLC-grade THF (Aldrich) and spectrograde chloroform (Fisher). Stock solutions with concentrations close to coil overlap were prepared gravimetrically by direct addition of polymer and solvent and filtered through 0.45- $\mu\text{m}$  filters (Rainin) into scrupulously dedusted light scattering cells. Dilute solutions were then prepared by direct addition of filtered solvent (0.2  $\mu\text{m}$  filters), and the cells flame-sealed. Higher concentration solutions were prepared in a two-step process. First, dilute benzene solutions were filtered into scattering cells and then freeze-dried until all the benzene was removed. In the second step, the appropriate amount of filtered solvent was added to the dry polymer, and the cells were sealed. Each solution also contained a small amount (0.2-0.5% relative to the polymer) of the antioxidant 2,6-di-*tert*-butyl-4-methylphenol (BHT). Solutions were allowed a lengthy period for equilibration, as there have been suggestions that anomalous "slow modes" in block copolymer solutions have diminished in intensity, or even vanished, over a time scale of weeks or months.<sup>17,18,20,21</sup> Accordingly, the most concentrated solutions were annealed for periods of at least 3 months. The ranges of weight fractions,  $w$ , covered for the four samples were 0.00039-0.55 for SI(16-19), 0.00051-0.36 for SI(41-45), 0.001-0.31 for SI(73-73), and 0.00062-0.23 for SI(170-170) and thus included the dilute, semidilute, and concentrated regimes. In addition, the concentration range extended beyond the order-disorder transition (ODT) for all four samples. Exact ODT conditions (*i.e.*,  $w$  and  $T$ ) were determined by static birefringence measurements, following the procedure of Balsara *et al.*,<sup>35</sup> as will be discussed elsewhere.<sup>36</sup> For solutions at 30.0 °C, the values of  $w_{\text{ODT}}$  were 0.520, 0.311, 0.260, and 0.140, for the four copolymers in order of increasing molecular weight. Solution concentrations,  $c$ , in units of g/mL, or volume fractions,  $\phi$ , were determined by assuming additivity of volumes and densities of 1.05, 0.913, and 0.867 g/mL for PS, PI, and toluene, respectively.

**Dynamic Light Scattering Measurements.** The DLS measurements were performed on a Malvern Model PCS-100 photogoniometer, in combination with a Lexel 95-2 Ar<sup>+</sup> laser operating at 488 nm, an ITT FW-130 photomultiplier, and a 264-channel multisample time correlator (Brookhaven Instru-

ments BI-2030AT). For each solution, intensity correlation functions  $g^{(2)}(q, t)$  were obtained at seven scattering angles from  $45^\circ$  to  $135^\circ$ , and it was established that in all cases the decays extended to the theoretical base line (typically within 0.1%, and always within 0.5%). Using the assumption of homodyne scattering and the Siegert relation,<sup>7,8</sup> the field correlation functions  $g^{(1)}(q, t)$  were obtained and analyzed by the Laplace inversion program CONTIN.<sup>37</sup> Representative examples of the intensity correlation functions and inversions will be presented in the Results section. All measurements were made with the temperature maintained at  $30.0 \pm 0.1^\circ\text{C}$ .

Measurements of the temporal distribution of scattered intensity on some of the solutions hinted that, as the ODT is approached, the scattered electric field might be deviating from a Gaussian distribution and/or that the system was not ergodic over the experimental time scale. This could invalidate use of the Siegert relation and thus potentially compromise the extraction of  $g^{(1)}(q, t)$  from a homodyne experiment. Accordingly, a set of measurements were made on a recently constructed Fourier transform heterodyne dynamic light scattering (FTH-DLS) instrument. The detailed principles and implementation of this technique will be described elsewhere,<sup>38</sup> but it is based on the surface-sensitive light scattering photometer developed by Mazur and Chung.<sup>39</sup> The reference beam has an electric field component which has been shifted in frequency by a selectable amount (100 Hz in these measurements), using a pair of acousto-optic modulators in series; the scattered field is unshifted. The intensity incident on the photomultiplier, therefore, has a component oscillating at 100 Hz; after the Fourier transform is performed, the 100 Hz peak may be analyzed as a sum of Lorentzians, with line widths corresponding to the decay rates in eq 1.

**Pulsed-Field-Gradient NMR.** Polymer solutions were flame-sealed under vacuum in 7-mm-o.d. NMR tubes and stored in the dark for at least 2 months prior to use. Center-of-mass diffusion measurements were performed using the large-pulsed-gradient spin-echo method, as described in detail elsewhere.<sup>40</sup> Nonspectroscopic pulsed  $^1\text{H}$  NMR was performed at 33 MHz in a conventional electromagnet, at a temperature of  $30.5 \pm 0.2^\circ\text{C}$ . The attenuation of the principal spin echo at  $2\tau = 50$  ms was measured as a function of the duration of the two field-gradient pulses, each following one of the two radio-frequency pulses in the  $90^\circ - \tau - 180^\circ - \tau$ -echo sequence. The field gradient,  $G$ , had a magnitude of 136, 383, or 585 Gauss/cm as required, each calibrated to within 1.5%. The pulse length  $\delta$ , was varied in 10–15 steps from 0 to 16 ms, or until the echo amplitude had decreased below 2% of its original value. At high  $G$  and large  $\delta$  we employed  $\delta$ -dependent differential gradient pulse length corrections to keep the echo centered at  $2\tau$  and compensated for receiver phase shifts.

A steady field gradient of  $G_0 = 0.85$  Gauss/cm was also applied throughout the on-resonance experiments. Some experiments at the lowest diffusion rates were repeated 3 kHz off-resonance in the single-side-band mode with  $G_0 = 0$ , recording the background-corrected integral of the magnitude Fourier transform centered on the echo, with results in agreement with the on-resonance mode. Each echo amplitude employed is the result of signal averaging over between 6 and 20 measurements. To aid in the interpretation of the diffusion spectrum, spin-spin relaxation ( $T_2$ ) measurements were performed on each specimen.

The echo-attenuation data were reduced off-line by a program which makes the required minor corrections for the effects of residual field gradients.<sup>41</sup> The fitted model postulated two separate, single diffusion rates, corresponding to solvent and polymer; the polymer polydispersity was too small to justify accounting for a distribution of diffusivities in the polymer contribution. The two observed attenuation rates were easily separated, as they differed by factors of between 50 and several thousand.

## Results

Typical Laplace inversions of the correlation functions by CONTIN are shown in Figure 1a–d, for the four

copolymers; the scattering angle is  $90^\circ$  throughout, and representative concentrations in the dilute, semidilute, and concentrated regimes are included. At each concentration, the height of the largest peak in the decay rate distribution,  $G(\Gamma)$ , has been normalized to unity, for convenient display; thus, comparisons of peak heights are significant only within a given curve. The following general observations may be made. For all four samples in the dilute regime, the distribution of decay rates is dominated by a single mode. This peak will be assigned to a superposition of  $\Gamma_C$  and  $\Gamma_H$ . Then, at concentrations near coil overlap, this peak broadens noticeably, as  $\Gamma_C$  and  $\Gamma_H$  begin to separate in time; by  $c \approx c^*$ , two modes are cleanly resolved. For the two lower molecular weights (Figures 1a and b),  $G(\Gamma)$  shows two well-resolved peaks through the semidilute and into the concentrated regimes. The faster mode increases in rate and decreases in relative amplitude, as  $c$  increases; this will be assigned to  $\Gamma_C$ . The slower mode decreases in rate and increases in relative amplitude, as  $c$  increases; this will be assigned to  $\Gamma_H$ . For the highest molecular weight (Figure 1d), the same features are evident, except that an additional, intermediate mode, appears for  $w = 0.049$  and persists at higher  $w$ . This mode will be assigned to  $\Gamma_I$ . Finally, for SI(73–73), there are consistently two modes throughout the semidilute regime, and some suggestions of a third, intermediate mode (see, for example the shoulder around  $5 \times 10^4 \text{ s}^{-1}$  for  $w = 0.178$ ); however, this third mode is not cleanly resolved. By the highest concentration shown, only  $\Gamma_H$  is well-defined; this data set corresponds to measurements taken on a solution in the ordered state. Representative intensity correlation functions, corresponding to the Laplace inversions in Figure 1d, are shown in Figure 2.

The angle dependence of each peak in  $G(\Gamma)$  was examined for all solutions, and for all modes assigned as  $\Gamma_C$  or  $\Gamma_H$ ,  $\Gamma \sim q^2$ . An example is shown in Figure 3, for SI(73–73) with  $w = 0.110$ . Thus, diffusion coefficients could be extracted unambiguously, as  $D = \Gamma/q^2$ . The angle dependence of  $G(\Gamma)$  is shown in Figure 4, for the SI(170–170) solution with  $w = 0.0489$ . Three peaks are consistently present in  $G(\Gamma)$ , and, at the lowest scattering angle ( $45^\circ$ ), there is a suggestion of a fourth, slower mode. However, such possible "slow modes" only occasionally appeared in the inversions; for example, comparing Figure 4 with Figure 1a–d, this data set is the exception, and we therefore assign no significance to this peak. The corresponding plots of  $\Gamma_C$ ,  $\Gamma_H$ , and  $\Gamma_I$  versus  $q^2$  are shown in Figure 5; it is evident that the fastest and slowest modes are diffusive, whereas the intermediate mode has, at most, a slight dependence on  $q$ . As  $qR_g$  is about 0.5 at  $q = 90^\circ$ , this increase in  $\Gamma_I$  with  $q$  could herald the crossover to the scaling  $\Gamma_I \sim q^4$  expected for the internal mode when  $qR_g \gg 1$ .<sup>9,10</sup>

The concentration dependences of  $D_C$  and  $D_H$  are shown for the four samples in Figure 6a–d, in double-logarithmic format. Also shown in each figure are the translational diffusivities,  $D_s$ , as obtained by NMR. From the close correspondence between  $D_s$  and  $D_H$ , it is clear that this mode indeed reflects translational diffusion. In Figure 6c, there is some discrepancy between  $D_s$  and  $D_H$  for SI(73–73) over the range  $0.05 \leq w \leq 0.1$ , for which we have no firm explanation. However, considering the results from all four samples together, the identity of this mode is clearly established. The factor in parentheses on the right-hand side of eq 10 predicts that  $D_H$  should fall increasingly below  $D_s$

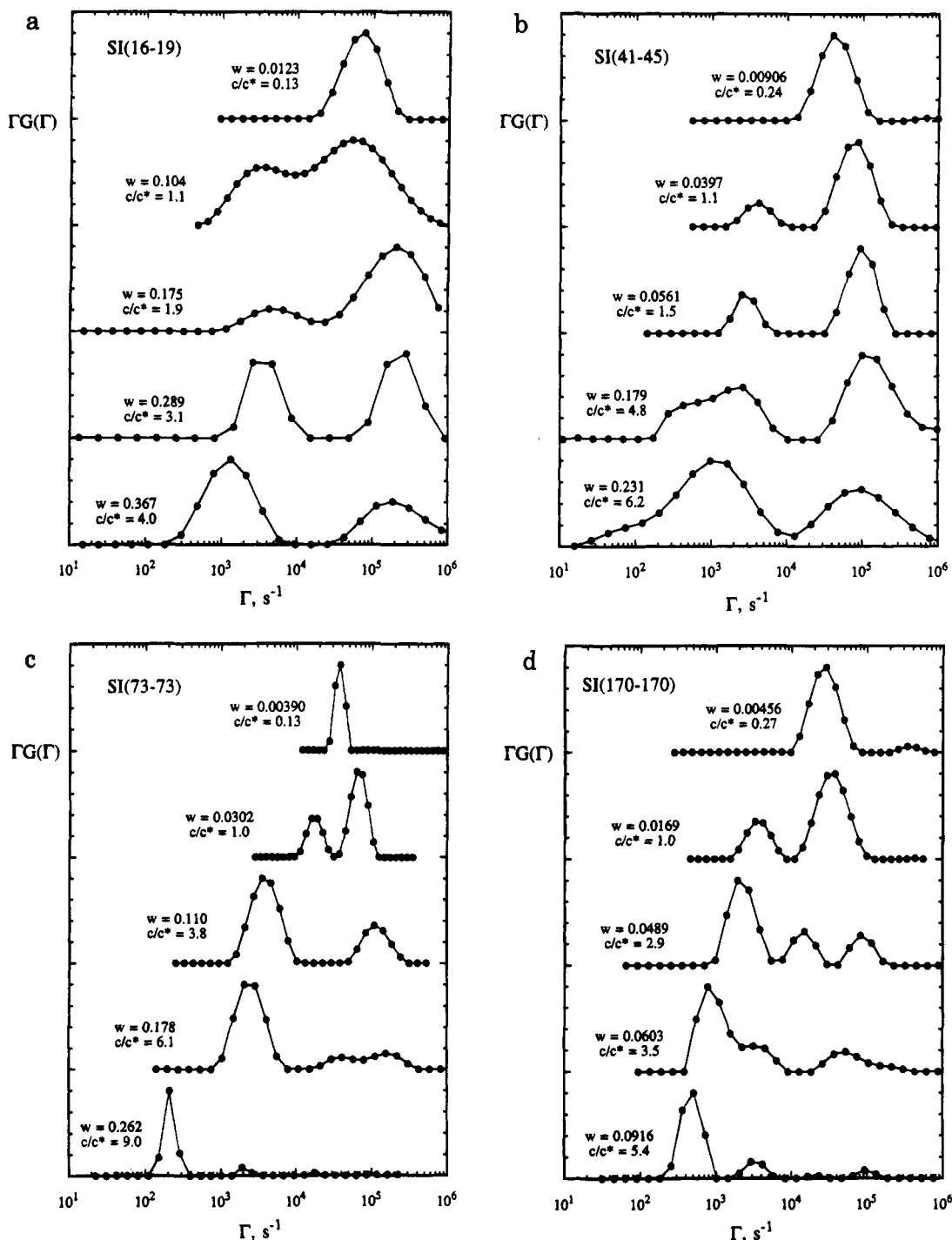


**Figure 1.** Laplace inversions of the correlation functions obtained at  $\theta = 90^\circ$  for (a) SI(16–19), (b) SI(41–45), (c) SI(73–73), and (d) SI(170–170) in toluene, at the indicated concentrations. The equal area representation,  $\Gamma G(\Gamma)$ , is used, and the smooth curves are intended as guides to the eye.

as  $c$  increases, but for these samples  $\kappa$  is sufficiently small that this correction should be at most 20%, which is certainly less than the combined uncertainties in  $D_s$  and  $D_H$ . It is interesting that the amplitude of the heterogeneity mode dominates the correlation functions, given that the samples are relatively narrowly distributed in molecular weight and thus presumably have limited compositional heterogeneity. However, it is important to recognize that this dominance is only evident for  $c > c^*$ , where the chain concentration is relatively high in the context of light scattering, and that  $A_H$  is predicted to increase linearly with  $c$ , whereas  $A_C$  should decrease with  $c$  in this regime.

The concentration dependence of  $D_C$  in Figure 6a–d is qualitatively as expected for cooperative diffusion:  $D_C$  increases slightly with  $w$  for  $c < c^*$ , and then more noticeably for  $c > c^*$ . Figure 7 presents the data in Figure 6a–d superposed in the scaling format,  $D/D_0$  vs  $c/c^*$ . The values of  $D_0$  were obtained by extrapolation of the dilute solution data to infinite dilution, which also yields values of the hydrodynamic radius,  $R_h$ , via the Stokes–Einstein relation:

$$D_0 = \frac{kT}{6\pi\eta_s R_h} \quad (12)$$

The resulting values of  $R_h$  are given in Table 1. The

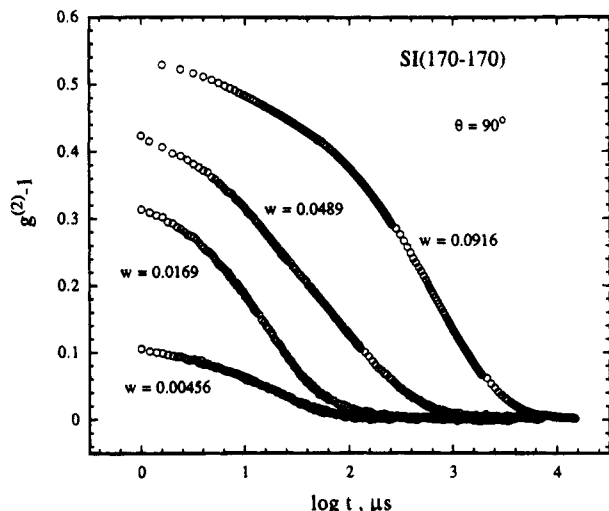


**Figure 2.** Intensity correlation functions underlying the Laplace inversions in Figure 1d.

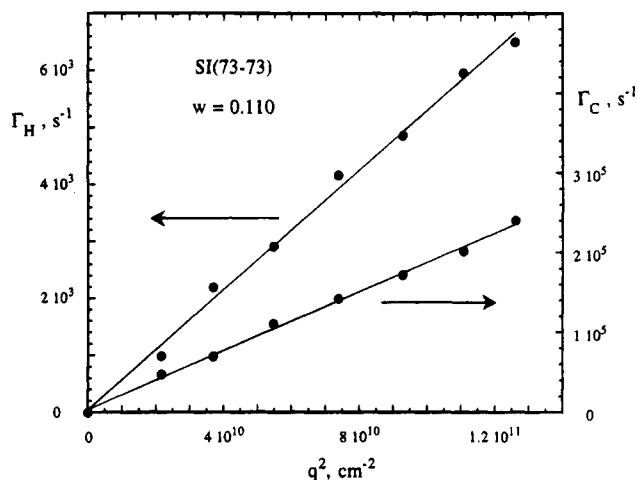


**Figure 3.** Angle dependence of the mean decay rate for the cooperative and heterogeneity modes, for SI(73-73) in toluene with  $w = 0.110$ .

values of  $c^*$  were calculated as

$$c^* = \frac{3M_w}{N_{av}4\pi R_g^3} \quad (13)$$

where  $R_g$  was estimated as  $1.3R_h$ . This plot reveals that  $D_H/D_0$  does not scale exactly with  $c/c^*$ , which is also the case for translational diffusion in homopolymers. On the other hand,  $D_C/D_0$  is sensibly independent of molecular weight, as expected for cooperative diffusion. A straight line drawn through the data for  $c/c^* > 1$  would give a slope of about 0.4, somewhat below the expected 0.75. However, this procedure could be misleading. To obtain a "correct" semidilute solution scaling exponent, one should satisfy the dual requirements of  $c/c^* > 1$  and  $c < 0.1$  g/mL, the latter being a generally-accepted cutoff, above which local friction effects and three-body interactions, etc., become important. Because the block copolymer molecular weights are relatively low, there are actually only a few data points that fall in the semidilute regime thus defined (2 for SI(45-45), 6 for SI(73-73), and 3 for SI(170-170)). If an exponent is extracted from these data alone, a value of 0.73 is obtained. This is illustrated in Figure 8, where  $D_C$  is plotted directly against  $w$ , and where a straight line has been fit to the semidilute data only (the filled symbols).

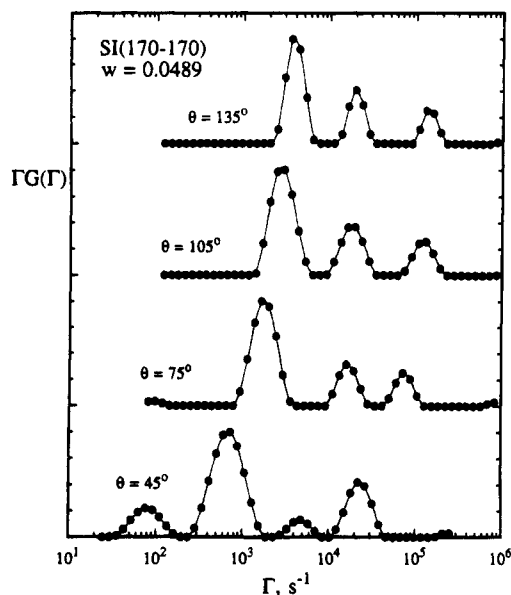


**Figure 4.** Laplace inversions of the correlation functions obtained at the indicated scattering angles, for SI(170-170) in toluene with  $w = 0.0489$ . The equal area representation,  $\Gamma G(\Gamma)$ , is used, and the smooth curves are intended as guides to the eye.

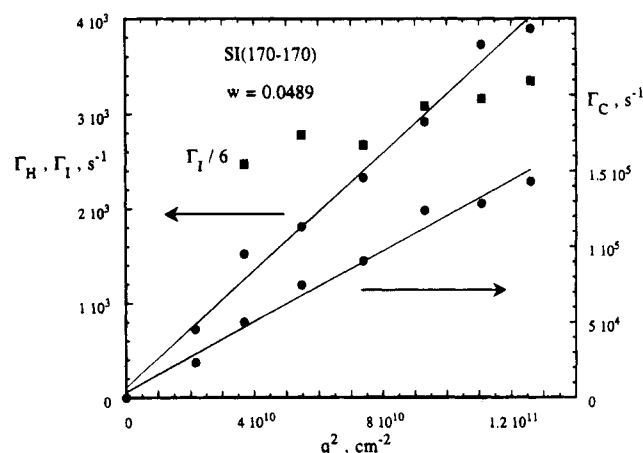


**Figure 5.** Angle dependence of the mean decay rate for the three modes observed for SI(170-170) in toluene with  $w = 0.0489$ . The decay rate for the intermediate mode has been divided by 6, to bring it onto the same scale.

At concentrations beyond 0.1, the data fall below this scaling, as also seen at higher concentrations in homopolymer solutions.<sup>42</sup> Thus, this mode is clearly confirmed as  $D_C$ ; furthermore, data for PS homopolymers in toluene<sup>32</sup> (not shown) are in quantitative agreement with these results, demonstrating that this mode is independent of chain architecture, as predicted.

The behavior of  $D_C$  and  $D_H$  described above is completely consistent with the predictions embodied in eqs 5, 6, and 10. However, the models also make testable predictions about the amplitudes of the modes, as in eqs 7, 8, and 11. Combining eqs 8 and 11, the prediction for the relative amplitude of the cooperative and heterogeneity modes in the semidilute regime is

$$(\langle n \rangle^2 - n_s^2)^2 \frac{A_H}{A_C} \frac{1}{N} \propto c^{1.25} \quad (14)$$

where the factor in the denominator on the right-hand side of eq 11 has been ignored. Figure 9 presents the data in this format, with a line of slope 1.25 drawn as

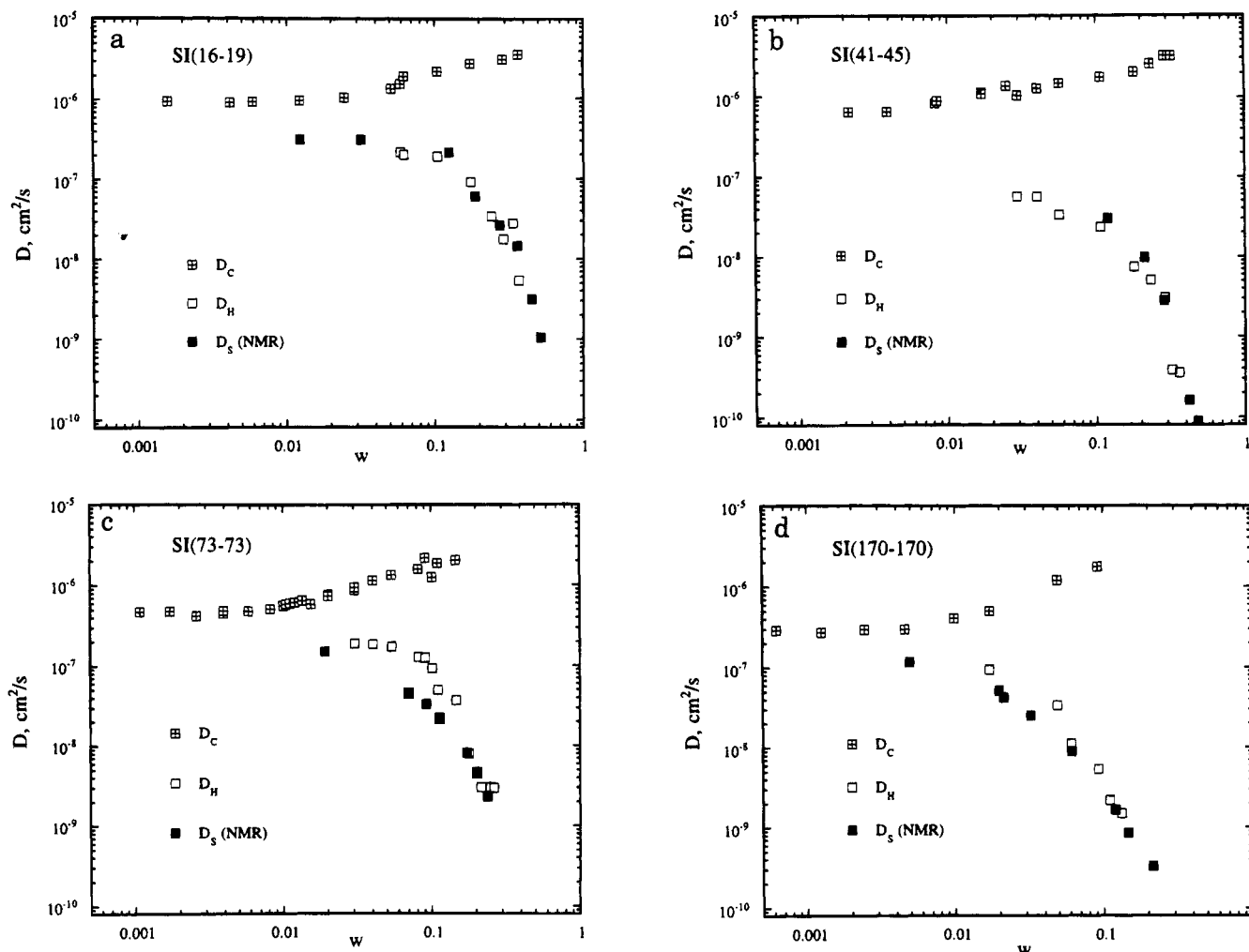


**Figure 6.** Concentration dependences of  $D_C$  and  $D_H$ , obtained by DLS, and  $D_s$ , obtained by NMR, for (a) SI(16-19), (b) SI(41-45), (c) SI(73-73), and (d) SI(170-170), in toluene.

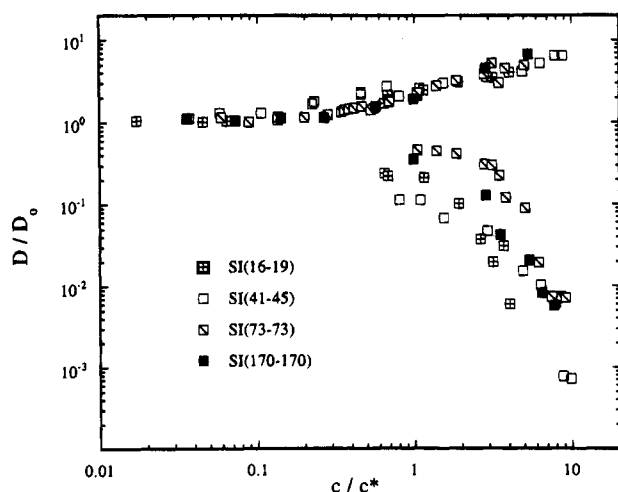


**Figure 7.** Scaling plot of reduced diffusivities,  $D_C/D_0$  and  $D_H/D_0$ , versus reduced concentration,  $c/c^*$ , for all four copolymers in toluene.

a guide to the eye. The reduction to a master curve is certainly not perfect, and data have been included for concentrations above 0.1 g/mL. Nevertheless, the predicted scaling of  $c^{1.25}$  is consistent with the data, given the uncertainty; the major source of uncertainty is in extracting the amplitudes of the modes via CONTIN, particularly when one of the modes contributes less than 10–20% of the total intensity. Measurements were also made for SI(73-73) in THF and chloroform, two other

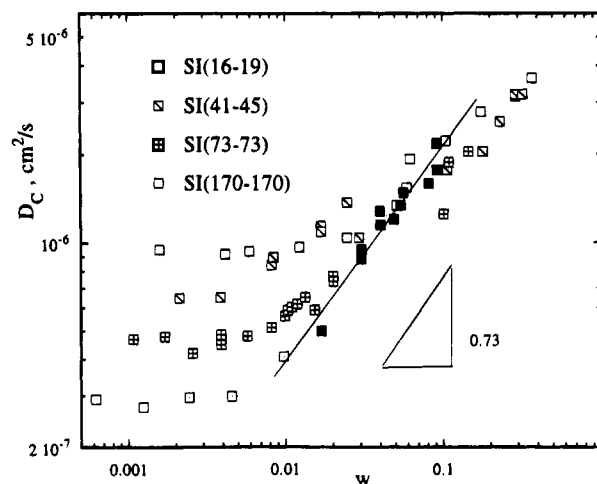


**Figure 8.** Concentration and molecular weight dependences of  $D_C$  for all four copolymers in toluene. The solid symbols denote data taken in the semidilute regime, which yield a concentration scaling exponent of 0.73.

good solvents with quite different refractive indices. Comparison of eqs 8 and 11 indicates that, as the solvent refractive index decreases,  $A_C$  should go up but  $A_H$  should be unchanged. Accordingly, the variation of  $n_s$  has been incorporated into eq 14 and into Figure 9, and this prediction is also supported by the data. As shown in Figure 10, the values of  $D_C$  and  $D_H$  are independent of solvent, as expected.

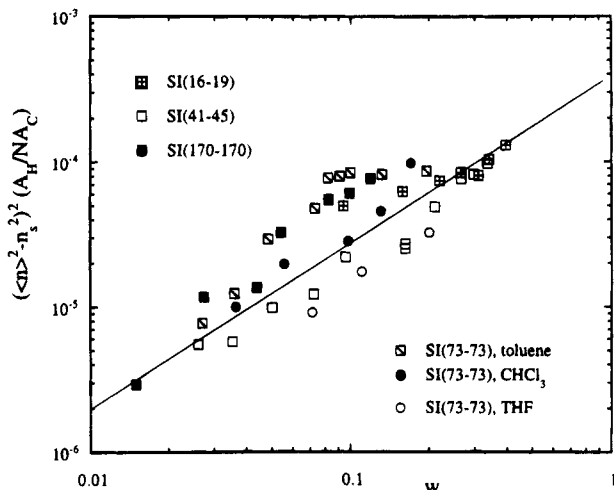


**Figure 9.** Relative amplitudes of the heterogeneity and cooperative modes, normalized according to eq 14, for all four copolymers in toluene, and for SI(73-73) in CHCl<sub>3</sub> and THF. The straight line has the predicted slope of 1.25 and is intended as a guide to the eye.

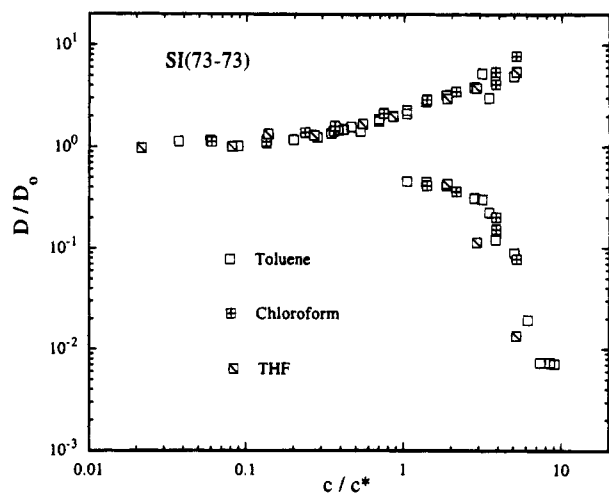


**Figure 10.** Concentration dependences of  $D_C$  and  $D_H$  for SI(73-73) in toluene, CHCl<sub>3</sub>, and THF.

The predicted internal mode was not generally observed, but with some confidence we can identify the intermediate mode seen for SI(170-170) at higher concentrations as  $\Gamma_I$ . The difficulty in resolving  $\Gamma_I$  can be attributed to several sources. First, it is almost always difficult to extract three modes from an experimental correlation function; they must be well-separated in time, yet comparable in amplitude. Second, the internal mode is predicted to have a low amplitude under most conditions. For example, in semidilute solutions, although  $A_C$  decreases,  $A_H$  should increase more rapidly than  $A_I$ , so it may be harder to find the internal mode for  $c \gg c^*$ ; this is consistent with our results. Also,  $A_I$  scales as  $M^2$  (for Gaussian chains), and block copolymers typically have relatively low  $M$ . Third,  $\Gamma_I$  is potentially close to  $\Gamma_C$  over a significant range of concentration. For example, in dilute solutions,  $\Gamma_I > \Gamma_C$ , whereas in semidilute solutions,  $\Gamma_C > \Gamma_I$ , so the two coincide near  $c^*$ .

The magnitude of  $\Gamma_I$  can be estimated from  $\Gamma_H$ , as follows. The Zimm, Rouse, and reptation theories all predict that the dimensionless ratio,  $D_s \tau_1 / R_g^2$ , should have a value of approximately 0.2.<sup>43</sup> Estimating  $R_g$  to be 13 and 21 nm for SI(73-73) and SI(170-170), respectively, yields estimates of  $\Gamma_I / \Gamma_H$  of 40 and 16 for

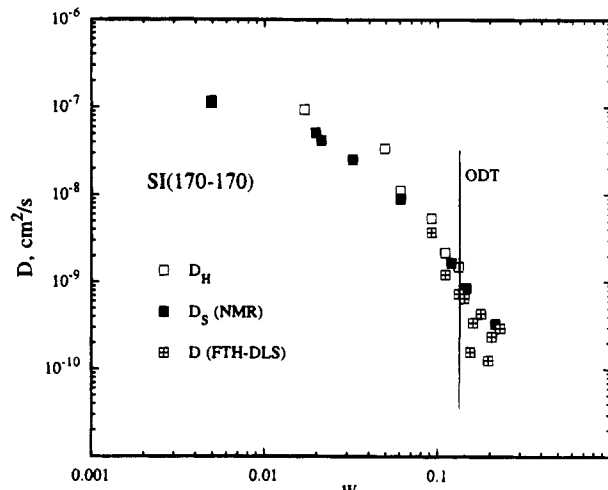


**Figure 11.** Concentration dependences of  $D_H$ , from homodyne DLS,  $D_s$ , from NMR, and  $D$  from Fourier transform heterodyne-DLS, for SI(170-170) in toluene. The data extend through the order-disorder transition and into the ordered state.

the two copolymers, respectively, independent of concentration, for a scattering angle of 90°. This separation is reasonably consistent with the results for SI(170-170) in Figures 1d and 4, where at  $\theta = 90^\circ$  the peaks assigned to  $\Gamma_I$  and  $\Gamma_H$  are separated by a factor of 10. However, rather than analyze the experimental correlation functions beyond the uncertainty inherent in Laplace inversion, we feel it is more appropriate to pursue the internal mode in more detail by using a zero-average-contrast solvent and thereby making  $A_C \approx 0$ . Under such circumstances, there should be at most two visible modes; this expectation has recently been confirmed.<sup>44</sup>

As noted in the Experimental Section, there is some concern that the scattered electric field is not a Gaussian random variable as the ODT is approached. In addition, separate measurements of polarized ( $I_{VV}$ ) and depolarized ( $I_{VH}$ ) scattered intensity for SI(170-170) indicated a net increase in both  $I_{VH}$  and  $I_{VV}$  as the ODT is approached;<sup>38</sup> the onset of this increase precedes the ODT as determined by static birefringence. The origin of this phenomenon is not clear, but one possibility is that it reflects the substantial concentration fluctuations, or regions of incipient lamellar order, that have been demonstrated by rheology and scattering from copolymer melts.<sup>2,3</sup> Recently, similar fluctuation effects have been seen by rheology and flow birefringence measurements on solutions of SI(73-73) on the disordered side of the ODT.<sup>45,46</sup> From a practical perspective, the issue is whether this phenomenon compromises the analysis of the correlation functions via the Siegert relation. To pursue this issue, we utilized the FTH-DLS instrument described briefly in the Experimental Section. Measurements were made on solutions of SI(73-73) ranging in concentration from  $w = 0.09$  to 0.23, and the resulting diffusion coefficients are shown in Figure 11. Note that, at these concentrations, the amplitude of the cooperative mode in the homodyne experiments is almost negligible, so that the correlation functions are effectively unimodal. From Figure 11 it is apparent that the FTH-DLS data agree well with the NMR measurements, albeit with some scatter. The values of  $D_H$  extracted by FTH-DLS appear to be comparable, or possibly slightly below, those obtained by DLS in the homodyne mode. On the basis of these preliminary measurements, therefore, we are inclined

to consider the homodyne results to be reliable at least up to the ODT, bearing in mind the inevitable experimental uncertainties with such concentrated systems. In addition,  $D_H$  passes smoothly through the ODT ( $w = 0.140$ ), as noted previously in solutions<sup>16,47</sup> and melts.<sup>48–51</sup>

### Comparison with Other Studies

Over the past 3 years eight papers have appeared describing DLS measurements on nearly-symmetric block copolymers in neutral good solvents.<sup>15–22</sup> The character of the modes observed and the tentative interpretations advanced vary considerably. However, we believe it is now possible to place almost all of these results within the common framework described in the Background section; this retrospective was greatly facilitated by the recent theoretical work of Semenov *et al.*<sup>13</sup>

The majority of the data are consistent with the existence of four distinct dynamic modes that have the following character:

(i) Cooperative diffusion ( $\Gamma_C = q^2 D_C$ ), which corresponds to translational diffusion only at infinite dilution and which increases in rate with increasing concentration.

(ii) An internal or structural mode ( $\Gamma_I$ ), which should be  $q$ -independent for small  $qR_g$  and  $q$ -dependent at higher  $q$ . At low  $qR_g$ ,  $\Gamma_I$  should correspond to the inverse longest relaxation time of the chain. In dilute solutions, this mode is faster than cooperative diffusion, but in semidilute solutions, it should cross over and become slower than cooperative diffusion. It is expected to have low amplitude for low molecular weights.

(iii) A heterogeneity mode ( $\Gamma_H \approx q^2 D_s$ ), dominated by translational diffusion of the chains, which should become resolvable from cooperative diffusion above  $c \approx c^*$ ; it is the slowest mode predicted by theory.

(iv) An additional, still slower mode, of unknown origin. It appears to involve cooperative motions of clusters of chains, but its complete characterization remains elusive.

In general, any given experimental correlation function should not be expected to detect all four modes, or even three, given that the conditions would have to be carefully chosen so that all of the modes have comparable amplitudes but distinct decay rates.

Five of the aforementioned papers appeared in 1991. Borsali *et al.*<sup>15</sup> examined a PS-PMMA diblock ( $M_w = 7.8 \times 10^5$ ,  $f_{PS} = 0.4$ ) in toluene for  $c \approx 5c^*$ . Two modes were clearly evident, and both decay rates were roughly  $q^2$ -dependent; in addition, the faster mode was quite comparable to  $D_C$  for a PS homopolymer solution. The interpretation of the slower mode was uncertain, because it was diffusive, and thus did not fit the character of the expected internal mode. However, we can now say that the magnitude (*ca.*  $7 \times 10^{-8}$  cm<sup>2</sup>/s) is close to that expected for translational diffusion. For example, Kent *et al.* report that  $D = 5 \times 10^{-8}$  cm<sup>2</sup>/s for a nearly symmetric PS-PMMA diblock with  $M_w = 8.9 \times 10^5$  at the same solution concentration.<sup>52</sup> In short, we may conclude that Borsali *et al.*<sup>15</sup> observed  $D_C$  and  $D_H$ , with  $\Gamma_I$  presumably unresolvable because it should overlap  $D_C$  for this concentration (and  $D_C$  and  $D_H$  were only a factor of 5 apart).

Duval and coworkers presented two studies of PS-PMMA in toluene, one<sup>18</sup> with  $M_w = 6.4 \times 10^5$  and the other<sup>17</sup> with  $M_w = 3.4 \times 10^5$ . The former study involved one concentration,  $c = 1.6c^*$ , and two modes were seen. The slower mode was diffusive and numerically consis-

tent with  $D_C$ . The faster mode was attributed to  $\Gamma_I$ . The latter study included a range of semidilute concentrations, and two diffusive modes were seen. The faster was again  $D_C$ , but the slower was attributed to "superstructures". However, its magnitude and concentration dependence are consistent with  $D_H$ , and this seems the more likely interpretation. The higher  $M_w$  and lower concentration in the former study presumably account for the observation of  $\Gamma_I$  and not  $\Gamma_H$ . These workers also noted the presence of an even slower mode that disappeared over time and that was more apparent at higher concentrations.

Konak and Podesva<sup>20</sup> examined a PS-PI diblock in diphenylethylene, with  $M_w = 1.8 \times 10^5$  and  $f_{PS} = 0.58$ ; four concentrations up to  $c = 8c^*$  were employed. They saw two modes and attributed the faster to  $\Gamma_I$  and the slower to  $D_C$ , based on the  $q$ -dependence. However, the magnitude of the slower mode ( $(3-6) \times 10^{-8}$  cm<sup>2</sup>/s) is at least an order of magnitude too low for  $D_C$  and is therefore more likely to reflect  $D_H$ , even though it increased slightly with concentration. Indeed, this sample is not too different from our SI(73-73), and comparison of the data in Figure 6c shows that over the relevant range ( $w = 0.01-0.06$ ) their slow mode is actually slightly below our  $D_H$ . Thus, it appears that these measurements found  $\Gamma_I$  and  $\Gamma_H$ , but not  $\Gamma_C$ . They also noted the appearance of a still slower mode, particularly at high concentrations.

Balsara *et al.*<sup>16</sup> in this laboratory examined a PS-PI diblock in toluene, with  $M_w = 3.1 \times 10^4$ ; five rather high concentrations were employed ( $w = 0.08-0.60$ ). As a consequence of this wide concentration range, these were the first DLS measurements to traverse the ODT. Two modes were consistently seen, with the faster mode diffusive and the slower close to  $q^3$ -dependent. Comparison with forced Rayleigh scattering and NMR measurements led the authors to suggest that the diffusive mode corresponded to translational diffusion, a then-novel speculation that now has theoretical and experimental support. Interestingly, the diffusivity was apparently unaffected by the ODT, in agreement with more recent results in melts<sup>48–51</sup> and the results presented here. The slower mode was attributed to dynamics of incipient grains, especially as it was found to slow down dramatically near the ODT. It is worth noting that these solutions were measured within a few days of their preparation, in contrast to those employed here. Consequently, and consistent with some of the other results above, we attribute the "slow mode" to a nonequilibrium state. The absence of  $\Gamma_I$  and  $\Gamma_C$  in the work of Balsara *et al.*<sup>16</sup> is now also straightforward to explain: it is a consequence of the low molecular weight and high concentrations involved.

More recently, there have been two other relevant studies. Tsunashima *et al.*<sup>22</sup> examined a PS-PMMA diblock ( $M_w = 1.5 \times 10^6$ ) in very dilute benzene solutions. Two modes were seen, the slower clearly identified as  $D_C$  and the faster possibly  $\Gamma_I$ ; the latter interpretation was uncertain because a  $q$ -independent regime was not detected as  $q \rightarrow 0$ . However, as the authors pointed out, the asymmetry of the sample ( $f_{PS} = 0.39$ ) can compromise the simple assignment of modes in the mean-field theory. Konak *et al.*<sup>21</sup> also examined a PS-PMMA diblock in toluene, but with low  $M_w$  ( $8 \times 10^4$ ) and higher concentration ( $w = 0.005-0.04$ ). The faster mode observed was consistent with  $D_C$ , but the slower mode, which was also diffusive, was ascribed to aggregation induced by crystallization of stereoregular

sequences on the PMMA chains. In support of this interpretation, the mode was found to disappear in chloroform, a better solvent for PMMA, and to be reduced in amplitude at higher temperature. However, it should be pointed out that the magnitude of this diffusion coefficient ( $4 \times 10^{-8} \text{ cm}^2/\text{s}$ ) is comparable to  $D_H$  (cf. SI(41–45) in Figure 6b) and that switching to chloroform would reduce the relative amplitude  $A_H/A_C$  by a factor of about 2.3, which might account for its “disappearance” ( $A_H/A_C$  was only about 0.3 in toluene). Of course, this interpretation does not explain the results of changing temperature; this issue perhaps should receive more experimental attention.

In a recent study that in many respects parallels our own, Jian *et al.*<sup>19</sup> examined the DLS properties of two PS–PI copolymers in toluene. One sample was asymmetric, but the other was symmetric with a total molecular weight of  $1.6 \times 10^6$ ; the latter specimen, therefore, is quite comparable to SI(73–73). Their results are quite consistent with ours, in the main. They find three modes and attribute them to  $\Gamma_C$ ,  $\Gamma_H$ , and  $\Gamma_I$ . The magnitudes and  $q$ -dependences are also comparable to those we report. There are two salient differences between their results and those reported here. First, Jian *et al.*<sup>19</sup> were able to resolve  $\Gamma_I$  cleanly for this polymer, in both dilute and concentrated solutions, whereas we could not. The origin of this difference is not clear. One possibility is that, in our case, the compositional heterogeneity was slightly higher, leading to a larger  $A_H$  that served to make the internal mode harder to resolve; another possibility is their use of a logarithmically-spaced correlator. The second difference is that Jian *et al.*<sup>19</sup> found the extra slow mode consistently, whereas we do not. As our correlation functions decayed to the theoretical base line, this difference is probably not related to hardware. They interpreted the mode as being due either to clusters of copolymer chains or to long-range density fluctuations; we feel our results are evidence that this mode is indicative of a nonequilibrium, or possibly metastable, state.

The above discussion summarizes the previous DLS measurements on block copolymers in neutral good solvents. However, as mentioned at the outset, there have been related studies using neutron scattering. The internal mode was, in fact, first cleanly observed by Borsali *et al.*,<sup>53</sup> using neutron spin echo on a concentrated solution of a PS–perdeutero-PS diblock. They blended benzene and perdeutero-benzene to achieve the zero-average-contrast condition noted in the Background section. The SANS  $q$  range enabled these workers to demonstrate the Rouse-like character of the internal mode. A follow-up study extended the measurements to three other concentrations,<sup>54</sup> but the conclusions were unchanged.

## Summary

The dynamic light scattering (DLS) from dilute, semidilute, and concentrated solutions of four nearly symmetric PS–PI diblock copolymers has been examined, in the neutral good solvent toluene. In dilute solutions, the distribution of decay rates was dominated by a single mode, whereas in semidilute and concentrated solutions, two modes were generally seen. Some supporting measurements were performed in THF and chloroform. Measurements of copolymer translational diffusion by NMR were also conducted. The results were interpreted in terms of the theories of Benmouna

*et al.*<sup>9,10</sup> and Semenov.<sup>13</sup> Finally, the results were compared with all of the previously-reported DLS measurements on block copolymers in nondilute neutral solutions.<sup>15–22</sup> It is argued that the apparent discrepancies among the previous studies can now be resolved. The specific conclusions are as follows:

1. A cooperative diffusion mode,  $D_C$ , was consistently seen. In the semidilute regime,  $D_C \sim c^{0.7}M^0$ , in agreement with theory and in agreement with measurements on homopolymer solutions. The amplitude of this mode decreased with increasing concentration and varied with solvent refractive index, as predicted.

2. A heterogeneity mode,  $D_H$ , was consistently seen for solution concentrations above coil overlap. Comparison with NMR results established the identity of this mode, which was only recently predicted by Semenov;<sup>13</sup> it is visible due to compositional heterogeneity in the copolymer chains, and it reflects translational diffusion. The amplitude of this mode also showed the predicted increase with concentration.

3. The concentration dependence of the translational diffusivity was unaffected by the order–disorder transition (ODT), as reported previously for solutions and melts. Measurements with a new Fourier transform heterodyne–DLS instrument both above and below the ODT gave values of  $D_H$  in substantial agreement with those from NMR and homodyne DLS.

4. The predicted internal mode could only be resolved cleanly for the highest molecular weight sample, and then only in the semidilute regime.

5. A fourth, even slower mode, that has been reported previously by several workers, was not consistently seen; it is proposed that this mode is indicative of a nonequilibrium state.

6. A detailed reexamination of previous measurements on similar systems suggests that  $D_H$  was consistently observed in those studies but incorrectly assigned; only in the study of Balsara *et al.*<sup>16</sup> was this mode attributed to translational diffusion. The recent theory of Semenov<sup>13</sup> therefore serves to reconcile a variety of apparent contradictions in the literature.

**Acknowledgment.** This work was supported in part by the National Science Foundation, through Grant DMR-9018807 (T.P.L.) and through Grant CHE-9203173 from the NSF Division of International Programs (a U.S.–Czech Cooperative Research award to T.P.L. and P.S.). In addition, the work was supported by the Center for Interfacial Engineering, an NSF-supported Engineering Research Center at the University of Minnesota, and by an NSF-REU award (W.M.). Helpful suggestions from G. Fytas and S. H. Anastasiadis are also gratefully acknowledged, as is the suggestion by a referee to employ the terminology “heterogeneity mode”.

## References and Notes

- (1) Almdal, K.; Rosedale, J. H.; Bates, F. S.; Wignall, G. D.; Fredrickson, G. H. *Phys. Rev. Lett.* **1990**, *65*, 1112.
- (2) Bates, F. S.; Rosedale, J. H.; Fredrickson, G. H. *J. Chem. Phys.* **1990**, *92*, 6255.
- (3) Rosedale, J. H.; Bates, F. S. *Macromolecules* **1990**, *23*, 2329.
- (4) Hajduk, D. A.; Harper, P. E.; Gruner, S. M.; Honeker, C.; Kim, G.; Thomas, E. L.; Fetters, L. J. *Bull. Am. Phys. Soc.* **1994**, *39* (1), 436.
- (5) Hamley, I. W.; Koppi, K. A.; Rosedale, J. H.; Bates, F. S.; Almdal, K.; Mortensen, K. *Macromolecules* **1993**, *26*, 5959.
- (6) Khandpur, A. K.; Forster, S.; Bates, F. S. *Bull. Am. Phys. Soc.* **1994**, *39* (1), 437.
- (7) Chu, B. *Laser Light Scattering*, 2nd ed.; Academic Press: San Diego, 1991.

- (8) Berne, B. J.; Pecora, R. *Dynamic Light Scattering*; Wiley: New York, 1976.
- (9) Benmouna, M.; Duval, M.; Borsali, R. *J. Polym. Sci., Polym. Phys. Ed.* **1987**, *25*, 1839.
- (10) Benmouna, M.; Benoit, H.; Borsali, R.; Duval, M. *Macromolecules* **1987**, *20*, 2620.
- (11) Akcasu, A. Z.; Hammouda, B.; Lodge, T. P.; Han, C. C. *Macromolecules* **1984**, *17*, 759.
- (12) Akcasu, A. Z.; Benmouna, M.; Benoit, H. *Polymer* **1986**, *27*, 1935.
- (13) Semenov, A. N.; Fytas, G.; Anastasiadis, S. H. *Polym. Prepr. (Am. Chem. Soc., Div. Polym. Chem.)* **1994**, *35* (1), 618.
- (14) Pusey, P. N.; Fijnaut, H. M.; Vrij, A. *J. Chem. Phys.* **1982**, *77*, 4270.
- (15) Borsali, R.; Fischer, E. W.; Benmouna, M. *Phys. Rev. A* **1991**, *43*, 5732.
- (16) Balsara, N. P.; Stepanek, P.; Lodge, T. P.; Tirrell, M. *Macromolecules* **1991**, *24*, 6227.
- (17) Haida, H.; Lingelser, J. P.; Gallot, Y.; Duval, M. *Makromol. Chem.* **1991**, *192*, 2701.
- (18) Duval, M.; Haida, H.; Lingelser, J. P.; Gallot, Y. *Macromolecules* **1991**, *24*, 6867.
- (19) Jian, T.; Anastasiadis, S. H.; Semenov, A. N.; Fytas, G.; Adachi, K.; Kotaka, T. *Macromolecules* **1994**, *27*, 4762.
- (20) Konak, C.; Podesva, J. *Macromolecules* **1991**, *24*, 6502.
- (21) Konak, C.; Vlcek, P.; Bansil, R. *Macromolecules* **1993**, *26*, 3717.
- (22) Tsunashima, Y.; Kawamata, Y. *Macromolecules* **1993**, *26*, 4899.
- (23) Anastasiadis, S. H.; Fytas, G.; Vogt, S.; Fischer, E. W. *Phys. Rev. Lett.* **1993**, *70*, 2415.
- (24) Anastasiadis, S. H.; Fytas, G.; Vogt, S.; Gerharz, B.; Fischer, E. W. *Europhys. Lett.* **1993**, *22*, 619.
- (25) Vogt, S.; Jian, T.; Anastasiadis, S. H.; Fytas, G.; Fischer, E. W. *Macromolecules* **1993**, *26*, 3357.
- (26) Vogt, S.; Anastasiadis, S. H.; Fytas, G.; Fischer, E. W. *Macromolecules* **1994**, *27*, 4335.
- (27) Stepanek, P.; Lodge, T. P., manuscript in preparation.
- (28) Patel, S. S.; Takahashi, K. M. *Macromolecules* **1992**, *25*, 4382.
- (29) Lodge, T. P.; Schrag, J. L. *Macromolecules* **1982**, *15*, 1376.
- (30) Nemoto, N.; Kojima, T.; Inoue, T.; Kishine, M.; Hirayama, T.; Kurata, M. *Macromolecules* **1989**, *22*, 3793.
- (31) Wheeler, L. M.; Lodge, T. P. *Macromolecules* **1989**, *22*, 3399.
- (32) Kim, H.; Chang, T.; Yohanan, J. M.; Wang, L.; Yu, H. *Macromolecules* **1986**, *19*, 2737.
- (33) Akcasu, A. Z.; Nägele, G.; Klein, R. *Macromolecules* **1991**, *24*, 4408.
- (34) Akcasu, A. Z.; Tombakoglu, M. *Macromolecules* **1990**, *23*, 607.
- (35) Balsara, N. P.; Perahia, D.; Safinya, C. R.; Tirrell, M.; Lodge, T. P. *Macromolecules* **1992**, *25*, 3896.
- (36) Pan, C.; Zhao, J.; Lodge, T. P.; Bates, F. S., unpublished results.
- (37) Provencher, S. W. *Comput. Phys. Commun.* **1982**, *27*, 229.
- (38) Pan, C. Ph.D. Thesis, University of Minnesota, Minneapolis, MN, 1995.
- (39) Mazur, E.; Chung, D. S. *Physica* **1987**, *147A*, 387.
- (40) von Meerwall, E.; Burgan, R. D.; Ferguson, R. D. *J. Magn. Reson.* **1979**, *34*, 339.
- (41) von Meerwall, E.; Ferguson, R. D. *Comput. Phys. Commun.* **1981**, *21*, 421.
- (42) Brown, W.; Stepanek, P. *Macromolecules* **1991**, *24*, 5484.
- (43) Doi, M.; Edwards, S. F. *The Theory of Polymer Dynamics*; Clarendon Press: Oxford, U.K., 1986.
- (44) Liu, Z.; Pan, C.; Stepanek, P.; Lodge, T. P., submitted to *Macromolecules*.
- (45) Jin, X.; Lodge, T. P. *Polym. Prepr. (Am. Chem. Soc., Polym. Chem. Div.)* **1994**, *35* (1), 585.
- (46) Lodge, T. P.; Xu, X.; Jin, X.; Dalvi, M. C. *Makromol. Chem., Macromol. Symp.* **1994**, *79*, 87.
- (47) Balsara, N. P.; Eastman, C. E.; Foster, M. D.; Lodge, T. P.; Tirrell, M. *Makromol. Chem., Macromol. Symp.* **1991**, *45*, 213.
- (48) Dalvi, M. C.; Lodge, T. P. *Macromolecules* **1994**, *27*, 3487.
- (49) Dalvi, M. C.; Eastman, C. E.; Lodge, T. P. *Phys. Rev. Lett.* **1993**, *71*, 2591.
- (50) Ehlich, D.; Takenaka, M.; Hashimoto, T. *Macromolecules* **1993**, *26*, 492.
- (51) Shull, K. R.; Kramer, E. J.; Bates, F. S.; Rosedale, J. H. *Macromolecules* **1991**, *24*, 1383.
- (52) Kent, M. S.; Tirrell, M.; Lodge, T. P. *J. Polym. Sci., Polym. Phys. Ed.* **1994**, *32*, 1927.
- (53) Borsali, R.; Benoit, H.; Legrand, J.-F.; Duval, M.; Picot, C.; Benmouna, M.; Farago, B. *Macromolecules* **1989**, *22*, 4119.
- (54) Duval, M.; Picot, C.; Benoit, H.; Borsali, R.; Benmouna, M.; Lartigue, C. *Macromolecules* **1991**, *24*, 3185.

MA9412041